GEOLOGY | THE GEOLOGICAL SOCIETY OF AMERICA®

https://doi.org/10.1130/G47343.1

Manuscript received 20 December 2019
Revised manuscript received 16 July 2020
Manuscript accepted 20 July 2020

Published online 25 August 2020

Rapid expansion of meso-megathermal rain forests into the southern high latitudes at the onset of the Paleocene-Eocene Thermal Maximum

E.P. Huurdeman[1], J. Frieling[2], T. Reichgelt[3], P.K. Bijl[2], S.M. Bohaty[4], G.R. Holdgate[5], S.J. Gallagher[6], F. Peterse[2], D.R. Greenwood[7] and J. Pross[1]*

[1]Institute of Earth Sciences, Heidelberg University, 69120 Heidelberg, Germany
[2]Department of Earth Sciences, Utrecht University, 3512 Utrecht, Netherlands
[3]Lamont-Doherty Earth Observatory, Columbia University, Palisades, New York 10964-8000, USA
[4]Ocean and Earth Science, University of Southampton, National Oceanography Centre, Southampton SO14 3ZH, UK
[5]Geotrack International, 37 Melville Road, Brunswick West, Victoria 3055, Australia
[6]School of Earth Sciences, University of Melbourne, Melbourne, Victoria 3053, Australia
[7]Biology Department, Brandon University, Brandon, Manitoba R7A 6A9, Canada

ABSTRACT

Current knowledge of terrestrial ecosystem response to the Paleocene-Eocene Thermal Maximum (PETM; ca. 56 Ma) is largely based on the midlatitudes of the Northern Hemisphere. To more fully reconstruct global terrestrial ecosystem response to the PETM, we generated vegetation and biomarker proxy records from an outcrop section on the southern coast of Australia (~60°S paleolatitude). We documented a rapid, massive, and sustained vegetation turnover as a response to regional PETM warming of ~1–4 °C, abruptly transitioning from a warm temperate to a meso-megathermal rain forest similar to that of present-day northeastern Queensland, Australia. The onset of this vegetation change preceded the characteristic PETM carbon-isotope excursion (CIE) by several thousand years. The reconstructed ecosystem change is much stronger than in other Southern Hemisphere records, highlighting the need for consideration of regional paleoceanographic, paleogeographic, and biogeographic characteristics to fully understand the global terrestrial ecosystem response to PETM climate forcing.

INTRODUCTION

The Paleocene-Eocene Thermal Maximum (PETM; ca. 56 Ma) was an ~200-k.y.-long hyperthermal event triggered by a massive injection of ^{13}C-depleted carbon into the atmosphere within 1–5 k.y. (Kirtland-Turner et al., 2017). Due to the rapidity of the carbon injection, the onset of the PETM represents a paleo-analog to current climate change, albeit occurring over a few thousand rather than a few hundred years (Foster et al., 2018). Thus, temporally well-resolved paleovegetation data from the PETM can help us to understand terrestrial ecosystem dynamics in response to atmospheric CO_2 increase and associated climate change. Previous work has shown that the PETM regionally triggered plant migrations and, to various extents, extirpations and originations (e.g., Wing et al., 2005; Jaramillo et al., 2010). However, current knowledge of PETM-induced vegetation change is strongly skewed toward the Northern Hemisphere, where the megafloral record from the Bighorn Basin (Wyoming, USA) in particular has yielded detailed insight into the vegetation response to increased CO_2 and rapid warming (Wing et al., 2005; Wing and Currano, 2013). In contrast, the terrestrial ecosystem response to PETM warming in the Southern Hemisphere is largely unknown, as available floral records are of low temporal resolution (Ocean Drilling Program [ODP] Site 1172, East Tasman Plateau; Contreras et al., 2014) or are from geographically isolated islands (New Zealand; e.g., Crouch and Brinkhuis, 2005; Handley et al., 2011).

Here, we present a detailed vegetation record for the latest Paleocene to earliest Eocene (ca. 56.1–55.9 Ma) based on sporomorphs from a high-deposition-rate, nearshore marine setting in southern Australia. With a paleolatitude of ~60°S (van Hinsbergen et al., 2015), our record resolves vegetation change during the initiation and peak of the PETM for the first time at a high-southern-latitude site. Our pollen- and biomarker-based temperature estimates provide further insight into the temporal relationships between terrestrial ecosystem change and PETM-related environmental forcing.

MATERIAL AND METHODS

Site Description

Situated on the southern coast of Australia near Princetown, Victoria (38°43′28.8″S, 143°10′35.0″E; Fig. 1), the Point Margaret outcrop exposes Upper Paleocene–Lower Eocene prodelta deposits of the Pember Mudstone of the Dilwyn Formation (Holdgate and Gallagher, 2003). We studied an interval of the Pember Mudstone spanning the PETM onset and extending into the body of the PETM carbon isotope excursion (CIE; 47.0–52.3 m section height; Frieling et al., 2018). High carbon/nitrogen ratios throughout the study section indicate a dominance of terrestrial organic matter (OM) and minimal influence of OM sourcing on the bulk organic $\delta^{13}C$ signal (Frieling et al., 2018). Sporomorphs and biomarkers at Point Margaret likely derive from proximal lowland, near-coastal settings, based on the lack of marked paleorelief in the hinterland (Joyce, 1992), the depositional setting off a river mouth (Holdgate and Gallagher, 2003), and the fact that river transport is responsible for most sporomorphs deposited in nearshore marine settings (Farley, 1987).

*E-mail: joerg.pross@geow.uni-heidelberg.de

CITATION: Huurdeman, E.P., et al., 2020, Rapid expansion of meso-megathermal rain forests into the southern high latitudes at the onset of the Paleocene-Eocene Thermal Maximum: Geology, v. 49, p. 40–44, https://doi.org/10.1130/G47343.1

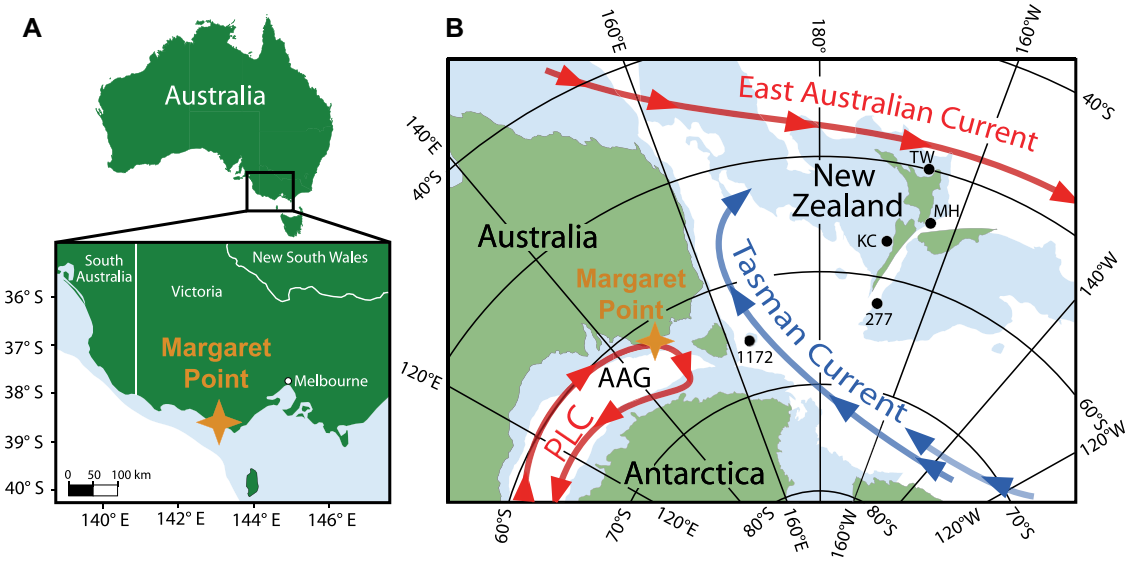

Figure 1. (A) Location of Point Margaret outcrop within present-day Australia. Land mass is in green, and submerged continental crust <3000 m water depth is in blue. (B) Early Eocene paleogeography and paleoceanography of the southwest Pacific region with surface-water currents (warm and cool currents in red and blue, respectively) and locations mentioned in text. AAG—Australo-Antarctic Gulf, PLC—proto–Leeuwin Current, 1172—Ocean Drilling Program (ODP) Site 1172, 277—Deep Sea Drilling Project (DSDP) Site 277, KC—Kumara-2 (Handley et al., 2011), MH—Moeraki-Hampden (Crouch and Brinkhuis, 2005), TW—Tawanui (Crouch and Visscher, 2003). Figure is after Huber et al. (2004).

Palynology

Sporomorphs were studied in 26 samples (sampling resolution: 0.50–0.05 m) from Point Margaret. Palynological processing involved treatment with hydrochloric and hydrofluoric acids and sieving through a 10 µm mesh (Pross et al., 2012). At least 300 sporomorphs were counted per sample and identified to the species level.

Mean annual air temperatures (MAATs) were estimated from the sporomorph data using the nearest living relative (NLR) approach (Reichgelt et al., 2015; Greenwood et al., 2017). Generalists and relictual taxa were omitted, and the presence of particular taxa was considered insignificant when the abundance was <10th percentile. Probability-density distributions were calculated from the individual climatic ranges of the NLRs of the fossil taxa (Table S2 in the Supplemental Material[1]; Hijmans et al., 2005), and a maximum likelihood analysis was performed using the fossil data set (Greenwood et al., 2017).

Organic Geochemistry

Branched glycerol dialkyl glycerol tetraethers (brGDGTs) were analyzed in 54 samples. The polar fractions separated from total lipid extracts were analyzed for brGDGTs by high-performance liquid chromatography/mass spectrometry after Hopmans et al. (2016). Source-assessment parameters indicated strong dominance of soil- and peat-derived brGDGTs in the samples (see Text S1; Fig. S1), allowing calculation of MAATs following the methylation index of branched tetraethers (MBT'_{5me}) and soil-based transfer function of Naafs et al. (2017). The root mean square error of this function (±4.0 °C) is most relevant when comparing absolute temperatures between sites; the intrasite (i.e., sample-to-sample) error is much smaller (Peterse et al., 2012), giving confidence to more subtle trends in our record.

Relative Timing of Proxy-Signal Shifts

Cross-correlation functions were used to quantify the stratigraphic offset between the various proxy signals across the CIE onset. These analyses were employed in a manner similar to that in Frieling et al. (2019) (see also Text S2). The results of these analyses were used to interpret phase relationships among the $\delta^{13}C$ signal, brGDGT-derived temperature change, and vegetation turnover.

RESULTS AND DISCUSSION

Latest Paleocene to Earliest Eocene Vegetation at Point Margaret

Sporomorph assemblages are well preserved and highly diverse in all studied samples from the Point Margaret section (Fig. 2), and visual inspection and ordination techniques revealed three distinct assemblages (Fig. 3). Analysis of similarities (ANOSIM) yielded a strong dissimilarity between the late Paleocene and the PETM assemblages ($R = 0.99$; $p < 0.001$; $n = 9999$). The samples from the uppermost Paleocene to the onset of the PETM CIE (47.3–50.8 m) contained elements that are characteristic of today's mesothermal rain forests in New Caledonia, New Guinea, and New Zealand (Macphail et al., 1994). Based on the ecology of their NLRs (Table S2), *Podocarpus*, *Dacrydium* (both Podocarpaceae), and Araucariaceae formed the forest canopy, while Proteaceae, *Trimenia*, and ferns (Cyatheaceae, Gleicheniaceae, and parent plants of *Laevigatosporites* spp.) made up the understory. Sclerophyll Proteaceae and Ericaceae pollen indicates the presence of open areas with heath-like vegetation. Importantly, insect-pollinated taxa such as Arecaceae (palms), *Strasburgeria*, and *Xylomelum* are also present; their pollen dispersal in extant rain forests is typically <100 m (Bush and Rivera, 1998), confirming the interpretation that the sporomorphs were deposited close to their source area. Mesothermal conditions in the uppermost Paleocene (47.3–50.5 m) are supported by our pollen-based climate estimates, with NLR-based MAATs of 18.0 °C on average (standard error [SE]: 0.2 °C). Independently, the brGDGT proxy yielded an average MAAT of 21.7 °C (SE: 0.1 °C; Fig. 2).

The onset of the PETM CIE at 50.8 m is associated with extensive vegetation turnover from a mesothermal to a meso-megathermal rain forest (Fig. 2). Within a transitional interval between 50.9 and 51.3 m, meso- to megathermal trees and shrubs (e.g., *Austrobuxus*, *Gymnostoma*), ferns (e.g., *Todisporites*, *Pteris*, *Lygodium*), and the megathermal mangrove palm *Nypa* increase to up to 75% of the assemblage at the expense of *Podocarpus*/*Dacrydium* and Araucariaceae (Fig. 2). A fern-spore peak at 51.00–51.05 m suggests a brief stage of disturbed vegetation cover (Vajda et al., 2001) within this vegetation-turnover interval. During the peak CIE (above 51.2 m), NLR and brGDGT-based estimates yield average MAATs of 21.7 °C (SE: 0.2 °C) and 22.9 °C (SE: 0.1 °C), respectively, representing a warming of 3.7 °C (NLR) and 1.2 °C

[1]Supplemental Material. Table S1 (nearest living relatives of the encountered sporomorphs), Table S2 (climatic parameters and modern distribution of the nearest living relatives), Text S1 including Figure S1 (source of the encountered biomarkers), Text S2 (timing of individual proxy signals), and Figures S2 and S3 (plates with photographs of encountered sporomorphs). Please visit https://doi.org/10.1130/GEOL.S.12811796 to access the supplemental material, and contact editing@geosociety.org with any questions. Data used in this paper are also available in the Pangaea database (www.pangaea.de).

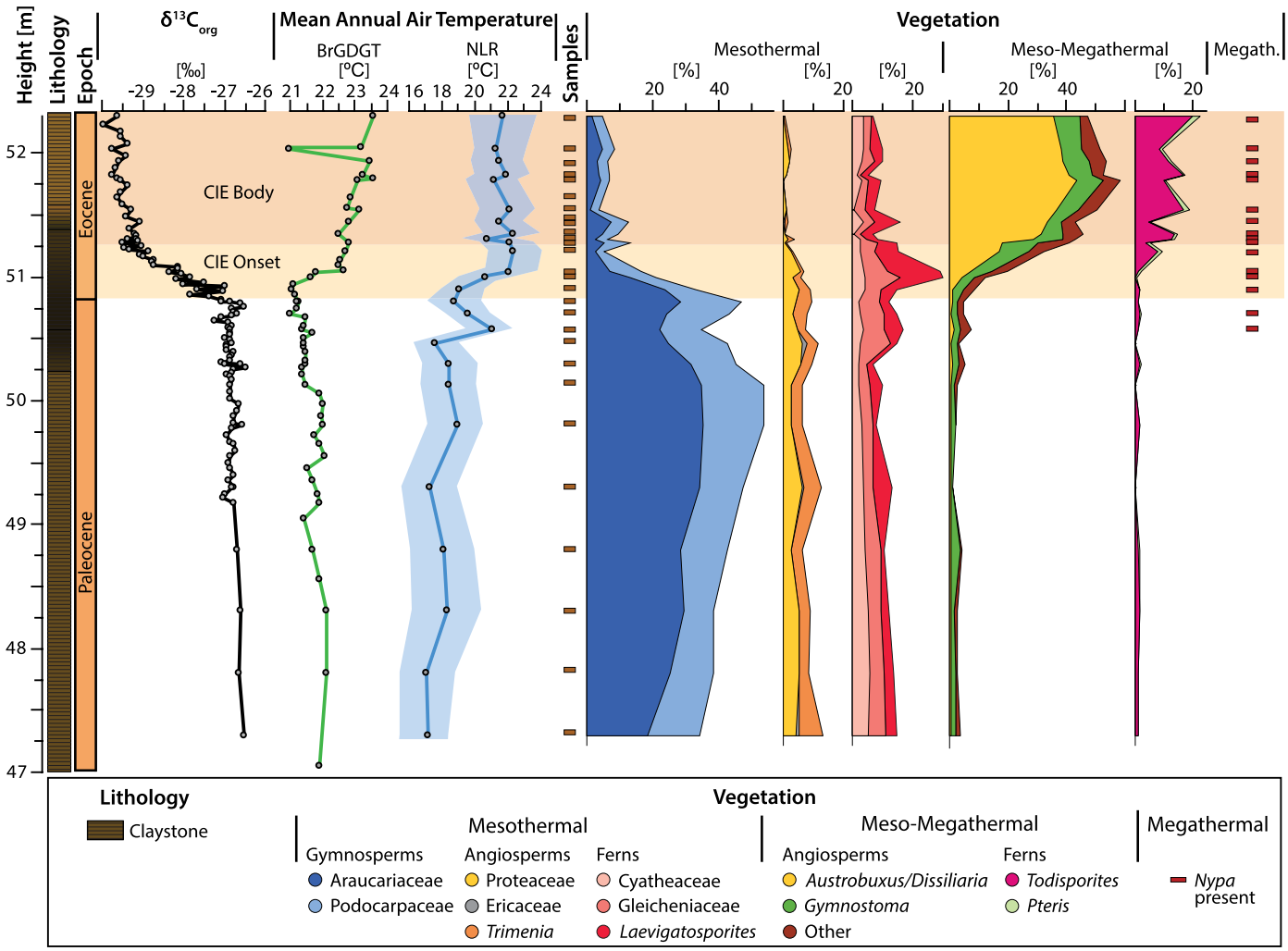

Figure 2. Selected sporomorph taxa from the uppermost Paleocene–lowermost Eocene at Point Margaret, Australia, grouped into mesothermal (14–20 °C), meso-megathermal (20–24 °C), and megathermal (>24 °C) elements, along with mean annual air temperature derived from organic geochemistry and palynology. Lithology and $\delta^{13}C_{org}$ data are from Frieling et al. (2018). Onset and body of carbon isotope excursion (CIE) are marked by shaded bars. NLR—nearest living relative; brGDGT—branched glycerol dialkyl glycerol tetraether.

(brGDGT) compared to the uppermost Paleocene baseline.

Terrestrial Ecosystem Response to PETM-Related Environmental Forcing

The high temporal resolution of our records, which is on the order of 1–3 k.y. for the PETM interval based on the available age control (Frieling et al., 2018), allows insight into the phase relationships between vegetation change and PETM-related environmental forcing. Megathermal taxa (e.g., *Nypa*) appear at 50.57 m, ~25 cm below the onset of the CIE (Fig. 2; see also Fig. S2). At the same stratigraphic level, the NLR-derived MAAT increases by ~3 °C. Cross-correlation function analysis of the NLR-based MAAT and $\delta^{13}C$ records suggests that the NLR-based warming leads the $\delta^{13}C$ shift in the depth domain by 5–10 cm (Fig. 4). Based on a mean sedimentation rate of ~7 cm/k.y. for the Point Margaret section (Frieling et al., 2018), the onset of vegetation-derived warming as documented by the advent of megathermal taxa therefore preceded the CIE by several (~1–4) thousand years.

Our data are the first to document a vegetation response to pre-CIE warming in the Southern Hemisphere, and the magnitude of the pollen-based, pre-CIE warming (NLR MAAT) is similar to that previously reported from marine (Thomas et al., 2002; Sluijs et al., 2007; Frieling

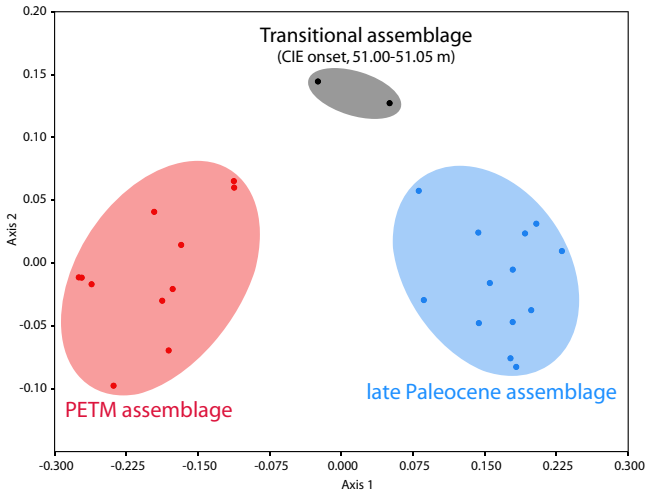

Figure 3. Nonmetric multidimensional scaling of Point Margaret (Australia) sporomorph assemblages, showing the first two axes of three-dimensional ordination using the Bray-Curtis dissimilarity index. Data were transformed by calculating square root and applying the Wisconsin Double transformation. Three distinctly different assemblages can be recognized (see text for details). PETM—Paleocene-Eocene Thermal Maximum.

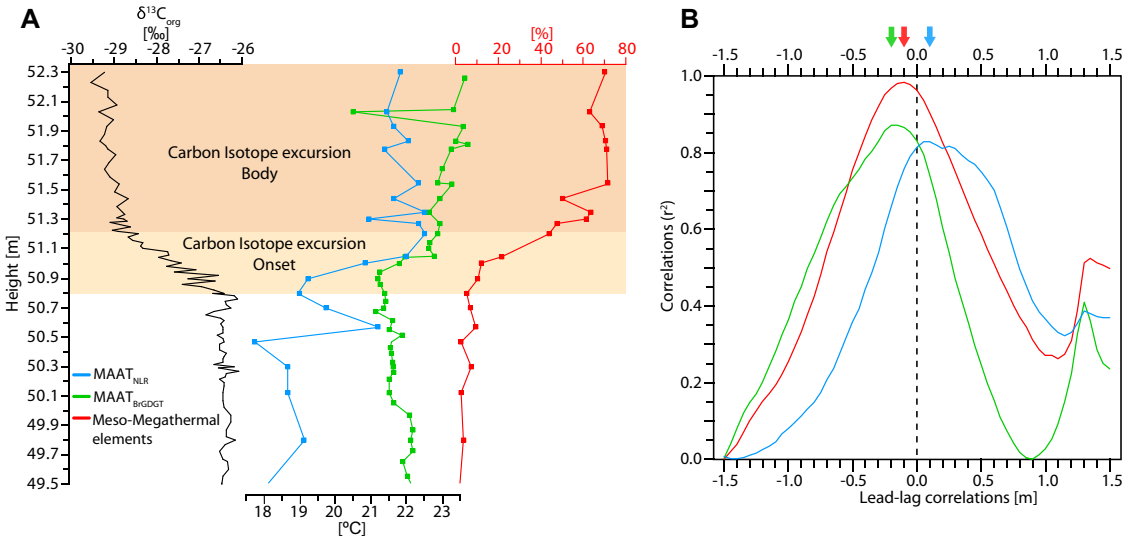

Figure 4. (A) Topmost ~3 m interval of Point Margaret (Australia) section showing $\delta^{13}C_{org}$ excursion, mean annual air temperature (MAAT) based on palynology and organic geochemistry, and percentage of meso-megathermal elements. Orange shading marks carbon isotope excursion (CIE). NLR—nearest living relative; brGDGT—branched glycerol dialkyl glycerol tetraether. (B) Correlation coefficients between $\delta^{13}C_{org}$ and $MAAT_{NLR}$, $MAAT_{brGDGT}$, and meso-megathermal elements, showing leads and lags in depth domain. Arrows mark positions of highest cross-correlation coefficients for each proxy (same color scheme as in A).

et al., 2019) and terrestrial records (Secord et al., 2010). Further analysis showed that brGDGT-derived MAAT increased after the CIE onset (at 51.1 m; Fig. 2) and lagged the $\delta^{13}C$ shift by 15–20 cm (Fig. 4). Quantitatively, the fraction of soil-derived OM, which carries the brGDGT MAAT signal, is likely low in Point Margaret sediments compared to the plant-derived OM fraction, which dominates the bulk $\delta^{13}C$ signal. Additionally, the elevated fern-spore abundance indicates disturbed vegetation cover within the PETM transition interval. The apparent lag in soil warming relative to the CIE onset may therefore have resulted from delivery of a mixture of contemporaneous and older eroded soil material, as similarly interpreted in other shallow-marine PETM sequences (Schneider-Mor and Bowen, 2013; see also Text S2).

Supraregional Vegetation and Temperature Change Across the PETM

The meso-megathermal rain-forest biome that was established at Point Margaret during the PETM contained numerous meso- to megathermal taxa typical of modern subtropical–tropical environments in Australia, New Caledonia, and New Guinea. In Australia, the closest extant analog to this biome is the coastal tropical rain forest of northeastern Queensland at a latitude of ~15°S (AVH, 2018). Hence, climate conditions during the PETM facilitated the growth of similar vegetation ~45° latitude farther south than today.

Although the coastal lowlands of southern Australia likely provided migration corridors for the expansion of thermophilous plant taxa to the Point Margaret region, lowland migration cannot explain the conspicuously early arrival of the mangrove palm *Nypa* at Point Margaret, which predated colonization by all other megathermal taxa (Fig. 2). In contrast to other megathermal elements, *Nypa* seeds are water dispersed (Tomlinson, 1986). During the Paleogene, the southwestern and southern coasts of Australia were bathed by the proto–Leeuwin Current, which originated in the lower latitudes (Fig. 1; Huber et al., 2004). The early *Nypa* appearance may thus have resulted from a favorable surface-current configuration, allowing direct transport of seeds from lower-latitude settings. *Nypa* is known from Paleocene strata of northwest Australia (Macphail and Hill, 2018), where it co-occurs with several other meso-megathermal elements (*Anacolosa*, Arecaceae, *Austrobuxus*, *Gymnostoma*, and Strasburgeriaceae) that also appear at Point Margaret during the PETM, further supporting such a scenario.

The PETM-induced increase in meso-megathermal elements at Point Margaret is much stronger than at ODP Site 1172 in the southwest Pacific Ocean (Fig. 1; Contreras et al., 2014). This may be due to the (1) paleogeographic position of the Point Margaret section, which allowed rapid immigration of meso-megathermal plant taxa from more northerly, pre-PETM habitats via lowland migration corridors, and/or (2) favorable paleoceanographic conditions in the Australo-Antarctic Gulf. In contrast, Site 1172 was located within the northward-flowing Tasman Current, which bathed southeastern Antarctica before reaching eastern Tasmania (Fig. 1; Huber et al., 2004). Thus, the sporomorphs at Site 1172 were likely sourced from catchment areas on Tasmania and the Antarctic margin, thereby representing an integrated vegetation signal that includes a wide spectrum of different, mostly cooler climate conditions between ~62°S and 72°S (Fig. 1; van Hinsbergen et al., 2015). Despite the appearance of *Nypa*, vegetation change in New Zealand was relatively minor during the PETM (e.g., Crouch and Visscher, 2003; Handley et al., 2011). This may be attributable to a diminished regional temperature response (Frieling et al., 2017) and the geographical isolation of New Zealand, which hampered rapid colonization by immigrant taxa (Wing and Currano, 2013).

Our MAAT estimates for the southern Australian coast also pose a challenge for supraregional terrestrial-marine integration of PETM temperature histories and circulation reconstructions. This problem is exemplified by inferred sea-surface temperatures at ODP Site 1172 and Deep Sea Drilling Project (DSDP) Site 277 (Fig. 1), which are ~10 °C warmer (~32–33 °C; Sluijs et al., 2011; Hollis et al., 2015) than MAATs at Point Margaret during the PETM (~21–23 °C; Fig. 2). These differences are likely due to as-yet-unexplained biases in the biotic and geochemical temperature proxies (Contreras et al., 2014) and require attention in future studies.

CONCLUSIONS

Our new data from Point Margaret in southern Australia (~60°S paleolatitude) reveal extensive vegetation turnover from a warm temperate to a meso-megathermal rain forest in conjunction with the PETM, accompanied by ~1–4 °C warming. This terrestrial ecosystem reorganization was much stronger than previously recognized in the Southern Hemisphere. Southern Australia may have been particularly prone to short-term climate-induced vegetation turnover due to the presence of coastal lowland migration corridors and coast-parallel surface currents originating in the lower latitudes. This underscores the assertion that a spatially differentiated perspective, including associated boundary conditions, is required in order to fully understand

terrestrial ecosystem change in response to past and future rapid climate forcing.

ACKNOWLEDGMENTS

We thank G. Dammers and C. Rem for laboratory assistance, and M. Huber, C. Jaramillo, and an anonymous reviewer for constructive feedback. Huurdeman and Pross acknowledge support by the German Research Foundation. Bijl and Greenwood acknowledge funding through Dutch Research Council (NWO) VENI and Natural Sciences and Engineering Research Council of Canada (NSERC) grants, respectively. Gallagher was supported by the Australian International Ocean Discovery Program (IODP) office and the Australian Research Council Basins Genesis Hub IH130200012.

REFERENCES CITED

Australasian Virtual Herbarium (AVH), 2018, The Australasian Virtual Herbarium: Council of Heads of Australasian Herbaria: http://avh.chah.org.au (accessed December 2018).

Bush, M.B., and Rivera, R., 1998, Pollen dispersal and representation in a neotropical rain forest: Global Ecology and Biogeography, v. 7, p. 379–392, https://doi.org/10.1046/j.1466-822x.1998.00293.x.

Contreras, L., Pross, J., Bijl, P.K., O'Hara, R.B., Raine, J.I., Sluijs, A., and Brinkhuis, H., 2014, Southern high-latitude terrestrial climate change during the Palaeocene–Eocene derived from a marine pollen record (ODP Site 1172, East Tasman Plateau): Climate of the Past, v. 10, p. 1401–1420, https://doi.org/10.5194/cp-10-1401-2014.

Crouch, E.M., and Brinkhuis, H., 2005, Environmental change across the Paleocene-Eocene transition from eastern New Zealand: A marine palynological approach: Marine Micropaleontology, v. 56, p. 138–160, https://doi.org/10.1016/j.marmicro.2005.05.002.

Crouch, E.M., and Visscher, H., 2003, Terrestrial vegetation record across the initial Eocene thermal maximum at the Tawanui marine section, New Zealand, *in* Wing, S.L., et al., eds., Causes and Consequences of Globally Warm Climates in the Early Paleogene: Geological Society of America Special Papers, v. 369, p. 351–364, https://doi.org/10.1130/0-8137-2369-8.351.

Farley, M.B., 1987, Palynomorphs from surface water of the eastern and central Caribbean Sea: Micropaleontology, v. 33, p. 254–262, https://doi.org/10.2307/1485641.

Foster, G.L., Hull, P., Lunt, D.J., and Zachos, J.C., 2018, Placing our current 'hyperthermal' in the context of rapid climate change in our geological past: Philosophical Transactions of the Royal Society: Mathematical, Physical, and Engineering Sciences, v. 376, p. 20170086, https://doi.org/10.1098/rsta.2017.0086.

Frieling, J., Gebhardt, H., Huber, M., Adekeye, O.A., Akande, S.O., Reichart, G.J., Middelburg, J.J., Schouten, S., and Sluijs, A., 2017, Extreme warmth and heat-stressed plankton in the tropics during the Paleocene-Eocene thermal maximum: Science Advances, v. 3, p. e1600891, https://doi.org/10.1126/sciadv.1600891.

Frieling, J., Huurdeman, E.P., Rem, C.C.M., Donders, T.H., Pross, J., Bohaty, S.M., Holdgate, G.R., Gallagher, S.J., McGowran, B., and Bijl, P.K., 2018, Identification of the Paleocene-Eocene boundary in coastal strata in the Otway Basin, Victoria, Australia: Journal of Micropalaeontology, v. 37, p. 317–339, https://doi.org/10.5194/jm-37-317-2018.

Frieling, J., Peterse, F., Lunt, D.J., Bohaty, S.M., Damsté, J.S., Reichart, G.J., and Sluijs, A., 2019, Widespread warming before and elevated barium burial during the Paleocene-Eocene thermal maximum: Evidence for methane hydrate release?: Paleoceanography and Paleoclimatology, v. 34, p. 546–566, https://doi.org/10.1029/2018PA003425.

Greenwood, D.R., Keefe, R.L., Reichgelt, T., and Webb, J.A., 2017, Eocene paleobotanical altimetry of Victoria's Eastern Uplands: Australian Journal of Earth Sciences, v. 64, p. 625–637, https://doi.org/10.1080/08120099.2017.1318793.

Handley, L., Crouch, E.M., and Pancost, R.D., 2011, A New Zealand record of sea level rise and environmental change during the Paleocene-Eocene thermal maximum: Palaeogeography, Palaeoclimatology, Palaeoecology, v. 305, p. 185–200, https://doi.org/10.1016/j.palaeo.2011.03.001.

Hijmans, R.J., Cameron, S.E., Parra, J.L., Jones, P.G., and Jarvis, A., 2005, Very high resolution interpolated climate surfaces for global land areas: International Journal of Climatology, v. 25, p. 1965–1978, https://doi.org/10.1002/joc.1276.

Holdgate, G., and Gallagher, S., 2003, Tertiary: A period of transition to marine basin environments, *in* Birch, W.D., ed., Geology of Victoria: Geological Society of Australia Special Publication 23, p. 289–335.

Hollis, C.J., Hines, B.R., Littler, K., Villasante-Marcos, V., Kulhanek, D.K., Strong, C.P., Zachos, J.C., Eggins, S.M., Northcote, L., and Phillips, A., 2015, The Paleocene-Eocene thermal maximum at DSDP Site 277, Campbell Plateau, southern Pacific Ocean: Climate of the Past, v. 11, p. 1009–1025, https://doi.org/10.5194/cp-11-1009-2015.

Hopmans, E.C., Schouten, S., and Damsté, J.S.S., 2016, The effect of improved chromatography on GDGT-based palaeoproxies: Organic Geochemistry, v. 93, p. 1–6, https://doi.org/10.1016/j.orggeochem.2015.12.006.

Huber, M., Brinkhuis, H., Stickley, C.E., Döös, K., Sluijs, A., Warnaar, J., Schellenberg, S.A., and Williams, G.L., 2004, Eocene circulation of the Southern Ocean: Was Antarctica kept warm by subtropical waters?: Paleoceanography, v. 19, PA4026, https://doi.org/10.1029/2004PA001014.

Jaramillo, C., et al., 2010, Effects of rapid global warming at the Paleocene-Eocene boundary on neotropical vegetation: Science, v. 330, p. 957–961, https://doi.org/10.1126/science.1193833.

Joyce, E.B., 1992, The West Victorian Uplands of southeastern Australia: Origin and history: Earth Surface Processes and Landforms, v. 17, p. 407–418, https://doi.org/10.1002/esp.3290170410.

Kirtland-Turner, S., Hull, P., Kump, L., and Ridgwell, A., 2017, A probabilistic assessment of the rapidity of the PETM onset: Nature Communications, v. 8, p. 353, https://doi.org/10.1038/s41467-017-00292-2.

Macphail, M.K., and Hill, R.S., 2018, What was the vegetation in northwest Australia during the Paleogene, 66–23 million years ago?: Australian Journal of Botany, v. 66, p. 556–574, https://doi.org/10.1071/BT18143.

Macphail, M.K., Alley, N.F., Truswell, E.M., and Sluiter, I.R.K., 1994, Early Tertiary vegetation: Evidence from spores and pollen, *in* Hill, R.S., ed., History of the Australian Vegetation: Cretaceous to Recent: Cambridge, UK, Cambridge University Press, p. 189–261, https://doi.org/10.20851/australian-vegetation.

Naafs, B.D.A., Gallego-Sala, A.V., Inglis, G.N., and Pancost, R.D., 2017, Refining the global branched glycerol dialkyl glycerol tetraether (brGDGT) soil temperature calibration: Organic Geochemistry, v. 106, p. 48–56, https://doi.org/10.1016/j.orggeochem.2017.01.009.

Peterse, F., van der Meer, J., Schouten, S., Weijers, J.W., Fierer, N., Jackson, R.B., Kim, J.H., and Sinninghe Damsté, J.S., 2012, Revised calibration of the MBT–CBT paleotemperature proxy based on branched tetraether membrane lipids in surface soils: Geochimica et Cosmochimica Acta, v. 96, p. 215–229, https://doi.org/10.1016/j.gca.2012.08.011.

Pross, J., et al., 2012, Persistent near-tropical warmth on the Antarctic continent during the early Eocene Epoch: Nature, v. 488, p. 73–77, https://doi.org/10.1038/nature11300.

Reichgelt, T., Kennedy, E.M., Conran, J.G., Mildenhall, D.C., and Lee, D.E., 2015, The early Miocene paleolake Manuherikia: Vegetation heterogeneity and warm- temperate to subtropical climate in southern New Zealand: Journal of Paleolimnology, v. 53, p. 349–365, https://doi.org/10.1007/s10933-015-9827-5.

Schneider-Mor, A., and Bowen, G.J., 2013, Coupled and decoupled responses of continental and marine organic-sedimentary systems through the Paleocene-Eocene thermal maximum, New Jersey margin, USA: Paleoceanography, v. 28, p. 105–115, https://doi.org/10.1002/palo.20016.

Secord, R., Gingerich, P.D., Lohmann, K.C., and MacLeod, K.G., 2010, Continental warming preceding the Palaeocene-Eocene thermal maximum: Nature, v. 467, p. 955–958, https://doi.org/10.1038/nature09441.

Sluijs, A., Brinkhuis, H., Schouten, S., Bohaty, S.M., John, C.M., Zachos, J.C., Reichart, G.J., Damste, J.S.S., Crouch, E.M., and Dickens, G.R., 2007, Environmental precursors to rapid light carbon injection at the Palaeocene/Eocene boundary: Nature, v. 450, p. 1218–1221, https://doi.org/10.1038/nature06400.

Sluijs, A., Bijl, P.K., Schouten, S., Röhl, U., Reichart, G.J., and Brinkhuis, H., 2011, Southern Ocean warming, sea level and hydrological change during the Paleocene-Eocene thermal maximum: Climate of the Past, v. 7, p. 47–61, https://doi.org/10.5194/cp-7-47-2011.

Thomas, D.J., Zachos, J.C., Bralower, T.J., Thomas, E., and Bohaty, S.M., 2002, Warming the fuel for the fire: Evidence for the thermal dissociation of methane hydrate during the Paleocene-Eocene thermal maximum: Geology, v. 30, p. 1067–1070, https://doi.org/10.1130/0091-7613(2002)030<1067:WTFFTF>2.0.CO;2.

Tomlinson, P.B., 1986, The Botany of Mangroves: Cambridge, UK, Cambridge University Press, 413 p.

Vajda, V., Raine, J.I., and Hollis, C.J., 2001, Indication of global deforestation at the Cretaceous-Tertiary boundary by New Zealand fern spike: Science, v. 294, p. 1700–1702, https://doi.org/10.1126/science.1064706.

van Hinsbergen, D.J., de Groot, L.V., van Schaik, S.J., Spakman, W., Bijl, P.K., Sluijs, A., Langereis, C.G., and Brinkhuis, H., 2015, A paleolatitude calculator for paleoclimate studies: PLoS One, v. 10, e0126946, https://doi.org/10.1371/journal.pone.0126946.

Wing, S.L., and Currano, E.D., 2013, Plant response to a global greenhouse event 56 million years ago: American Journal of Botany, v. 100, p. 1234–1254, https://doi.org/10.3732/ajb.1200554.

Wing, S.L., Harrington, G.J., Smith, F.A., Bloch, J.I., Boyer, D.M., and Freeman, K.H., 2005, Transient floral change and rapid global warming at the Paleocene-Eocene boundary: Science, v. 310, p. 993–996, https://doi.org/10.1126/science.1116913.

Printed in USA